Multidimensional Summation-By-Parts Operators: General Theory and Application to Simplex Elements[☆]

Jason E. Hicken[a,1,*], David C. Del Rey Fernández[b,2], David W. Zingg[b,3]

[a]*Department of Mechanical, Aerospace, and Nuclear Engineering,*
Rensselaer Polytechnic Institute,
Troy, New York, United States
[b]*Institute for Aerospace Studies,*
University of Toronto,
Toronto, Ontario, M3H 5T6, Canada

Abstract

Summation-by-parts (SBP) operators offer the efficiency of finite-difference methods with the provable time stability of Galerkin finite-element methods, but they have traditionally been limited to tensor-product domains. This paper presents a definition for multidimensional SBP finite-difference operators that is a natural extension of the classical one-dimensional SBP definition. Theoretical implications of the definition are investigated for the special case of a diagonal-norm (mass) matrix, and it is shown that the operators retain the desirable properties of tensor-product SBP operators. A cubature rule with positive weights is proven to be a necessary and sufficient condition for the existence of diagonal-norm SBP operators on a particular domain. Concrete examples of multidimensional SBP operators are constructed for the triangle and tetrahedron; similarities and differences with spectral-element and spectral-difference methods are discussed. An assembly process is described that builds diagonal-norm SBP operators on a global domain from element-level operators. Numerical results of linear advection on a doubly periodic domain demonstrate the accuracy and time stability of the simplex operators.

Keywords: summation-by-parts, finite-difference method, unstructured grid, spectral-element method, spectral-difference method, mimetic discretization

1. Introduction

Summation-by-parts (SBP) operators are high-order finite-difference schemes that mimic the symmetry properties of the differential operators they approximate [1]. Respecting such symmetries has important implications; in particular, they enable SBP discretizations that are both time-stable

---

[*]corresponding author

Email addresses: `hickej2@rpi.edu` (Jason E. Hicken), `dcdelrey@oddjob.utias.utoronto.ca` (David C. Del Rey Fernández), `dwz@oddjob.utias.utoronto.ca` (David W. Zingg)

[1]Assistant Professor
[2]Graduate Student
[3]Professor and Director

and high-order accurate [2–4], properties that are essential for robust, long-time simulations of turbulent flows [5, 6].

Most existing SBP operators are one-dimensional [7–10] and are applied to multidimensional problems using a multi-block tensor-product formulation [11–13]. Like other tensor-product methods, the restriction to multi-block grids complicates mesh generation and adaptation, and it limits the geometric complexity that can be considered in practice.

The limitations of the tensor-product formulation motivate our interest in generalizing SBP operators to unstructured grids. There are two ways this generalization has been pursued in the literature: 1) construct global SBP operators on an arbitrary distribution of nodes, or; 2) construct SBP operators on reference elements and assemble a global discretization by coupling these smaller elements.

While the first approach is appealing conceptually, it presents challenges. Kitson *et al.* [14] showed that, for a given stencil width and design accuracy, there exists grids for which no stable, diagonal-norm SBP operator exists. Thus, building stable high-order SBP operators on arbitrary node distributions may require unacceptably large stencils. When SBP operators do exist for a given node distribution, they must be determined globally by solving a system of equations, in general. The global nature of these SBP operators is exemplified in the mesh-free framework of Chiu *et al.* [15, 16].

The second approach — constructing SBP operators on reference elements and using these to build the global discretization — is more common and presents fewer difficulties. The primary challenge here is to extend the one-dimensional SBP operators of Kreiss and Scherer [1] to a broader set of operators and domains. The existence of such operators, at least in the dense-norm case[4], was established by Carpenter and Gottlieb [17]. They proved that operators with the SBP property can be constructed from the Lagrangian interpolant on nearly arbitrary nodal distributions, which is practically feasible on reference elements with relatively few nodes. More recently, Gassner [18] showed that the discontinuous spectral-element method is equivalent to a diagonal-norm SBP discretization when the Legendre-Gauss-Lobatto nodes are used with a lumped mass matrix.

Of particular relevance to the present work is the extension of the SBP concept by Del Rey Fernandez *et al.* [19]. They introduced a generalized summation-by-parts (GSBP) definition for arbitrary node distributions on one-dimensional elements, and these ideas helped shape the definition of SBP operators presented herein.

Our first objective in the present work is to develop a suitable definition for multi-dimensional SBP operators on arbitrary grids and to characterize the resulting operators theoretically. We note that the discrete-derivative operator presented in [15] is a possible candidate for defining (diagonal-norm) multi-dimensional SBP operators; however, it lacks properties of conventional SBP operators that we would like to retain, such as the accuracy of the discrete divergence theorem [20].

Our second objective is to provide a concrete example of multi-dimensional diagonal-norm SBP operators on non-tensor-product domains. We follow the element-based approach and construct SBP operators for triangular and tetrahedral elements. The resulting operators are similar to those used in the nodal triangular-spectral-element method [21–23]. Unlike the spectral-element method based on cubature points, we do not insist on a polynomial basis and use the resulting freedom to enforce the summation-by-parts property; this leads to provably time-stable schemes.

The remaining paper is structured as follows. Section 2 presents notation and the proposed definition for multi-dimensional SBP operators. We study the theoretical implications of the pro-

---

[4]In this paper, norm matrix is synonymous with mass matrix.

posed definition in Section 3. We then describe, in Section 4, how to construct diagonal-norm SBP operators for the triangle and tetrahedron. Section 4 also establishes that SBP operators on subdomains can be assembled into SBP operators on the global domain. Results of applying the triangular SBP operators to the linear advection equation are presented in Section 5. Conclusions are given in Section 6.

2. Preliminaries

To make the presentation concise, we concentrate on multi-dimensional SBP operators in two dimensions; the extension to higher dimensions follows in a straightforward manner. Furthermore, in many cases we present definitions and theorems for operators in the x coordinate direction only.

2.1. Notation

We consider discretized derivative operators defined on a set of n nodes, $S = \{(x_i, y_i)\}_{i=1}^n$. Capital letters with script type are used to denote continuous functions. For example, $\mathcal{U}(x) \in L^2(\Omega)$ denotes a square-integrable function on the domain Ω. We use lower-case bold font to denote the restriction of functions to the nodes. Thus, the restriction of $\mathcal{U}$ to S is given by

$$\boldsymbol{u} = [\mathcal{U}(x_1, y_1), \ldots, \mathcal{U}(x_n, y_n)]^\mathrm{T}. \tag{1}$$

Following this convention, the nodes themselves will often be represented by the two vectors $\boldsymbol{x} = [x_1, \ldots, x_n]^\mathrm{T}$ and $\boldsymbol{y} = [y_1, \ldots, y_n]^\mathrm{T}$. More generally, the restriction of monomials to S is represented by $\boldsymbol{x}^j = \left[x_1^j, \ldots, x_n^j\right]^\mathrm{T}$ and $\boldsymbol{y}^j = \left[y_1^j, \ldots, y_n^j\right]^\mathrm{T}$, with the convention that $\boldsymbol{x}^j = \boldsymbol{y}^j = \boldsymbol{0}$ if $j < 0$. We use the element-wise Hadamard product, denoted $\circ$, to represent the product of functions restricted to the nodes. For example, the restriction of $x^a y^b$ to S is given by $\boldsymbol{x}^a \circ \boldsymbol{y}^b$.

Matrices are represented using capital letters with sans-serif font; for example, the first derivative operators with respect to x and y are represented by the matrices D_x and D_y, respectively. Entries of a matrix are indicated with subscripts, and we follow Matlab®-like notation when referencing submatrices. For example, $\mathsf{A}_{:,j}$ denotes the jth column of matrix A, and $\mathsf{A}_{:,1:k}$ denotes its first k columns.

2.2. Multidimensional SBP operator definition

We propose the following definition for D_x, the SBP first-derivative operator with respect to x. An analogous definition holds for D_y and, in three-dimensions, D_z. Definition 1 is a natural extension of the definition of GSBP operators proposed in [19], which itself extends the classical SBP operators introduced by Kreiss and Scherer [1].

Definition 1. Two-dimensional summation-by-parts operators: *Consider an open and bounded domain $\Omega \subset \mathbb{R}^2$ with a piecewise-smooth boundary Γ. The matrix D_x is a degree p SBP approximation to the first derivative $\frac{\partial}{\partial x}$ on the nodes $S = \{(x_i, y_i)\}_{i=1}^n$ if*

i) $\mathsf{D}_x \boldsymbol{x}^{a_x} \circ \boldsymbol{y}^{a_y} = a_x \boldsymbol{x}^{a_x-1} \circ \boldsymbol{y}^{a_y}, \ \forall \, a_x + a_y \leq p$;

ii) $\mathsf{D}_x = \mathsf{H}^{-1}\mathsf{S}_x = \mathsf{H}^{-1}\left(\mathsf{Q}_x + \frac{1}{2}\mathsf{E}_x\right)$, *where Q_x is antisymmetric, and E_x is symmetric;*

iii) H *is symmetric positive definite, and;*

iv) $(\boldsymbol{x}^{a_x} \circ \boldsymbol{y}^{a_y})^\mathrm{T} \mathsf{E}_x \boldsymbol{x}^{b_x} \circ \boldsymbol{y}^{b_y} = \oint_\Gamma x^{a_x+b_x} y^{a_y+b_y} n_x \mathrm{d}\Gamma, \qquad \forall \, a_x + a_y, b_x + b_y \leq \tau_{\mathsf{E}_x},$

where $\tau_{\mathsf{E}_x} \geq p$ and $\boldsymbol{n} = [n_x, n_y]^\mathrm{T}$ is the outward pointing unit normal to the surface Γ.

3

Before studying the implications of Definition 1 in Section 3, it is worthwhile to motivate and elaborate on each of the four properties in the definition.

Property i ensures that D_x is an accurate approximation to the first-partial derivative with respect to x. It does this in the usual way by requiring that the operator be exact for polynomials of total degree less than or equal to p. Consequently, in two dimensions the minimum number of nodes necessary to satisfy property i is

$$n_{\min} = \frac{(p+1)(p+2)}{2}. \tag{2}$$

For d dimensions it is necessary to have at least $\binom{p+d}{d}$ nodes. Unlike finite-element methods, SBP operators generally need more nodes than required by the accuracy conditions, in order to satisfy properties ii–iv.

Property ii is needed for the SBP operator to mimic integration by parts (IBP). Recall that the IBP formula for the x derivative is

$$\int_\Omega \mathcal{V}\frac{\partial \mathcal{U}}{\partial x}\mathrm{d}\Omega = \oint_\Gamma \mathcal{V}\mathcal{U}n_x\mathrm{d}\Gamma - \int_\Omega \mathcal{U}\frac{\partial \mathcal{V}}{\partial x}\mathrm{d}\Omega,$$

where the outward-pointing unit normal to the surface is $\boldsymbol{n} = [n_x, n_y]^{\mathrm{T}}$. The SBP approximation of IBP follows immediately from property ii:

$$\boldsymbol{v}^{\mathrm{T}}\mathsf{H}\mathsf{D}_x\boldsymbol{u} = \boldsymbol{v}^{\mathrm{T}}\mathsf{E}_x\boldsymbol{u} - \boldsymbol{u}^{\mathrm{T}}\mathsf{H}\mathsf{D}_x\boldsymbol{v}, \qquad \forall\, \boldsymbol{v}, \boldsymbol{u} \in \mathbb{R}^n. \tag{3}$$

The matrix H must be symmetric positive-definite to guarantee stability: without property iii, the discrete "energy", $\boldsymbol{u}^{\mathrm{T}}\mathsf{H}\boldsymbol{u}$, could be negative when $\boldsymbol{u}^{\mathrm{T}}\boldsymbol{u} > 0$, and vice versa. The so-called norm matrix H can be interpreted as a mass matrix, i.e.

$$\mathsf{H}_{i,j} = \int_\Omega \phi_i(x)\phi_j(x)\mathrm{d}\Omega,$$

but it is important to emphasize that SBP operators are finite-difference operators, and there is no (known) closed-form expression for the basis $\{\phi_i\}_{i=1}^n$, in general. In the diagonal norm case, we shall show that another interpretation of H is as a cubature rule.

Finally, property iv implies that E_x is a degree τ_{E_x} approximation to the surface integral

$$\oint_\Gamma \mathcal{V}\mathcal{U}n_x\mathrm{d}\Gamma. \tag{4}$$

While property iv is not explicitly present in one-dimensional SBP definitions [1, 7], it is implicitly satisfied by tensor-product SBP operators [20]. For general domains, property iv must be explicitly enforced in order to approximate the surface integral in IBP accurately, and, consequently, retain desirable properties like dual consistency [24].

3. Analysis of diagonal-norm multi-dimensional summation-by-parts operators

In this section, we determine the implications of Definition 1 on the constituent matrices of a multi-dimensional SBP operator and whether or not such operators exist. The focus is on diagonal-norm operators; however, the ideas presented here can be extended to dense-norm operators, i.e. where the matrix H is not diagonal.

The following lemma will prove useful in the sequel. It follows immediately from properties i and ii, so we state it without proof.

Lemma 1 (compatibility). *Let* $\mathsf{D}_x = \mathsf{H}^{-1}(\mathsf{Q}_x + \frac{1}{2}\mathsf{E}_x)$ *be an SBP operator of degree p. Then we have the following set of relations:*

$$a_x \left(\boldsymbol{x}^{b_x} \circ \boldsymbol{y}^{b_y} \right)^{\mathrm{T}} \mathsf{H}\boldsymbol{x}^{a_x-1} \circ \boldsymbol{y}^{a_y} + b_x \left(\boldsymbol{x}^{a_x} \circ \boldsymbol{y}^{a_y} \right)^{\mathrm{T}} \mathsf{H}\boldsymbol{x}^{b_x-1} \circ \boldsymbol{y}^{b_y} =$$
$$\left(\boldsymbol{x}^{b_x} \circ \boldsymbol{y}^{b_y} \right)^{\mathrm{T}} \mathsf{E}_x \boldsymbol{x}^{a_x} \circ \boldsymbol{y}^{a_y}, \qquad a_x + a_y, b_x + b_y \leq p. \quad (5)$$

We refer to (5) as the compatibility equations for the x derivative; H must simultaneously satisfy analogous relations for E_y. The relation between H and E_x was first derived by Kreiss and Scherer [1] and Strand [7], to construct a theory for one-dimensional classical finite-difference-SBP operators. Furthermore, Del Rey Fernández *et al.* [19] have used these relations to extend the theory of such operators to a broader set. What is presented in this paper is a natural extension of those works to multi-dimensional operators, and the derivation of (5) follows in a straightforward manner from any of the mentioned works.

For diagonal-norm operators, meaning that H is a diagonal matrix, Definition 1 leads to the following:

Theorem 1. *Let* H *be the diagonal norm matrix associated with the SBP operators* D_x *and* D_y *of degree p on S. If* $\boldsymbol{u}, \boldsymbol{v} \in \mathbb{R}^n$ *are the restriction to S of smooth functions* $\mathcal{U}(x, y)$ *and* $\mathcal{V}(x, y)$, *respectively, then* $\boldsymbol{v}^{\mathrm{T}}\mathsf{H}\boldsymbol{u}$ *must must be at least a degree* $2p - 1$ *approximation to the integral inner product* $\int_\Omega \mathcal{V}\mathcal{U}\mathrm{d}\Omega$.

Proof. This result follows in an analogous fashion to the one-dimensional result, see Section 4.1 [19]. One starts with the compatibility equations for the x coordinate (5) and proves the result. It then follows that the compatibility equations for the y coordinate are also satisfied. $\qquad \square$

A direct consequence of Theorem 1 is

Corollary 1. *The nodal coordinates,* $S = \{(x_i, y_i)\}_{i=1}^n$, *and diagonal entries of* H *from a diagonal-norm SBP operator form a cubature rule with positive weights that is exact for polynomials of degree* $2p - 1$.

Now we prove the following:

Theorem 2. *Let* $n_{\min} = (p + 1)(p + 2)/2$ *be the dimension of the polynomial basis of degree p in two dimensions, and consider the node set* $S = \{(x_i, y_i)\}_{i=1}^n$ *with* $n \geq n_{\min}$ *nodes. Define the generalized Vandermonde matrix* $\mathsf{V} \in \mathbb{R}^{n \times n_{\min}}$ *whose columns are the monomial-basis elements evaluated at the nodes;*

$$\mathsf{V}_{:,k} = \boldsymbol{x}^i \circ \boldsymbol{y}^{j-i}, \qquad k = \frac{j(j+1)}{2} + i + 1, \quad \forall\, j = 0, 1, \ldots, p, \quad i = 0, 1, \ldots, j.$$

If the columns of V *are linearly independent, then the existence of a cubature rule of degree* $\tau_\mathsf{H} \geq 2p - 1$ *with positive weights is necessary and sufficient for the existence of degree p diagonal-norm SBP operators approximating the first derivatives* $\frac{\partial}{\partial x}$ *and* $\frac{\partial}{\partial y}$ *on the node set S.*

Proof. The necessary condition follows immediately from Theorem (1). To prove sufficiency, we must show that, given a cubature rule, we can construct an operator that satisfies properties i–iv of Definition 1 on the same node set as the cubature rule.

5

Before proceeding, we introduce some matrices that facilitate the proof. Let $\mathsf{V}_x \in \mathbb{R}^{n \times n_{\min}}$ be the matrix whose columns are the x derivatives of the monomial-basis:

$$(\mathsf{V}_x)_{:,k} = i\boldsymbol{x}^{i-1} \circ \boldsymbol{y}^{j-i}, \qquad k = \frac{j(j+1)}{2} + i + 1, \quad \forall \, j = 0, 1, \ldots, p, \quad i = 0, 1, \ldots, j.$$

We construct an invertible matrix $\tilde{\mathsf{V}} \in \mathbb{R}^{n \times n}$ by appending a set of linearly independent vectors, $\mathsf{W} \in \mathbb{R}^{n \times (n-n_{\min})}$, to V:

$$\tilde{\mathsf{V}} \equiv \begin{bmatrix} \mathsf{V} & \mathsf{W} \end{bmatrix}.$$

Similarly, we define

$$\tilde{\mathsf{V}}_x \equiv \begin{bmatrix} \mathsf{V}_x & \mathsf{W}_x \end{bmatrix},$$

where $\mathsf{W}_x \in \mathbb{R}^{n \times (n-n_{\min})}$ is an arbitrary matrix. Below, we use the degrees of freedom in W_x to satisfy the SBP definition.

Let H be the diagonal matrix whose entries are the cubature weights ordered consistently with the cubature node set S. Since the cubature weights are positive, property iii is satisfied.

Next, we use the cubature to construct a suitable E_x. Using V and V_x, we define the symmetric matrix

$$\tilde{\mathsf{E}}_x \equiv \mathsf{V}^{\mathrm{T}} \mathsf{H} \mathsf{V}_x + \mathsf{V}_x^{\mathrm{T}} \mathsf{H} \mathsf{V}.$$

Since V and V_x are polynomials of degree p and $p-1$, respectively, evaluated at the nodes, the cubature is exact for the right-hand side of $\tilde{\mathsf{E}}_x$:

$$\begin{aligned} \left(\tilde{\mathsf{E}}_x \right)_{k,l} &= \int_\Omega i x^{i-1} y^{j-i} x^q y^{r-q} \mathrm{d}\Omega + \int_\Omega q x^i y^{j-i} x^{q-1} y^{r-q} \mathrm{d}\Omega \\ &= \oint_\Gamma x^{i+q} y^{j-i+r-q} n_x \mathrm{d}\Gamma, \qquad \forall \, j, r = 0, 1, \ldots, p, \quad i = 0, 1, \ldots, j, \quad q = 0, 1, \ldots, r, \end{aligned}$$

where $k = j(j+1)/2 + i + 1$, and $l = r(r+1)/2 + q + 1$. To make the connection with property iv, let $a_x = i$, $a_y = j - i$, $b_x = q$ and $b_y = r - q$. Then,

$$\left(\tilde{\mathsf{E}}_x \right)_{k,l} = \oint_\Gamma x^{a_x + b_x} y^{a_y + b_y} n_x \mathrm{d}\Gamma, \qquad a_x + a_y = j \leq p, \quad b_x + b_y = r \leq p. \tag{6}$$

Now we can define the boundary operator

$$\mathsf{E}_x \equiv \tilde{\mathsf{V}}^{-\mathrm{T}} \begin{bmatrix} \tilde{\mathsf{E}}_x & \mathsf{F}^{\mathrm{T}} \\ \mathsf{F} & \mathsf{G} + \mathsf{G}^{\mathrm{T}} \end{bmatrix} \tilde{\mathsf{V}}^{-1},$$

where $\mathsf{F} \in \mathbb{R}^{(n-n_{\min}) \times n_{\min}}$ and $\mathsf{G} \in \mathbb{R}^{(n-n_{\min}) \times (n-n_{\min})}$ have arbitrary entries. It follows from this definition that E_x is symmetric. Moreover, together with (6), this definition implies

$$\left(\mathsf{V}^{\mathrm{T}} \mathsf{E}_x \mathsf{V} \right)_{k,l} = \left(\tilde{\mathsf{E}}_x \right)_{k,l} = \oint_\Gamma x^{a_x + b_x} y^{a_y + b_y} n_x \mathrm{d}\Gamma,$$

so E_x satisfies property iv.

Finally, let

$$\mathsf{Q}_x \equiv \mathsf{H} \tilde{\mathsf{V}}_x \tilde{\mathsf{V}}^{-1} - \frac{1}{2} \mathsf{E}_x. \tag{7}$$

The accuracy conditions, which are equivalent to showing $\mathsf{D}_x\mathsf{V} = \mathsf{V}_x$, follow immediately from this definition of Q_x:

$$\mathsf{D}_x\mathsf{V} = \mathsf{H}^{-1}\left(\mathsf{Q}_x + \frac{1}{2}\mathsf{E}_x\right)\mathsf{V} = \mathsf{H}^{-1}\left(\mathsf{H}\tilde{\mathsf{V}}_x\tilde{\mathsf{V}}^{-1}\right)\mathsf{V} = \mathsf{V}_x,$$

thus, property i is satisfied.

Our remaining task is to show that Q_x can be constructed to be antisymmetric; inspecting (7), we see that the W_x block of $\tilde{\mathsf{V}}_x$ provides the only available degrees of freedom to achieve this task. If we can show that

$$\tilde{\mathsf{V}}^{\mathrm{T}}\mathsf{Q}_x\tilde{\mathsf{V}} = \begin{bmatrix} \mathsf{V}^{\mathrm{T}}\mathsf{Q}_x\mathsf{V} & \mathsf{V}^{\mathrm{T}}\mathsf{Q}_x\mathsf{W} \\ \mathsf{W}^{\mathrm{T}}\mathsf{Q}_x\mathsf{V} & \mathsf{W}^{\mathrm{T}}\mathsf{Q}_x\mathsf{W} \end{bmatrix}$$

can be made antisymmetric, then the result will follow for Q_x. Consider the first block in the 2×2 block matrix above, i.e.

$$\mathsf{V}^{\mathrm{T}}\mathsf{Q}_x\mathsf{V} = \mathsf{V}^{\mathrm{T}}\mathsf{H}\mathsf{V}_x - \frac{1}{2}\mathsf{V}^{\mathrm{T}}\mathsf{E}_x\mathsf{V}.$$

Adding this block to its transpose, we find

$$\mathsf{V}^{\mathrm{T}}\mathsf{Q}_x\mathsf{V} + \mathsf{V}^{\mathrm{T}}\mathsf{Q}_x^{\mathrm{T}}\mathsf{V} = \mathsf{V}^{\mathrm{T}}\mathsf{H}\mathsf{V}_x + \mathsf{V}_x^{\mathrm{T}}\mathsf{H}\mathsf{V} - \mathsf{V}^{\mathrm{T}}\mathsf{E}_x\mathsf{V}, \tag{8}$$

where we have used the symmetry of E_x. The right-hand side of (8) is the matrix form of the (rearranged) compatibility equations (5). Thus, $\mathsf{V}^{\mathrm{T}}\mathsf{Q}_x\mathsf{V} + \mathsf{V}^{\mathrm{T}}\mathsf{Q}_x^{\mathrm{T}}\mathsf{V} = 0$, proving that the first block is antisymmetric. For the remaining three blocks, antisymmetry requires

$$\left(\mathsf{V}^{\mathrm{T}}\mathsf{Q}_x\mathsf{W}\right)^{\mathrm{T}} = -\mathsf{W}^{\mathrm{T}}\mathsf{Q}_x\mathsf{V}, \qquad \text{and} \qquad \mathsf{W}^{\mathrm{T}}\mathsf{Q}_x\mathsf{W} = -\mathsf{W}^{\mathrm{T}}\mathsf{Q}_x^{\mathrm{T}}\mathsf{W}.$$

Substituting Q_x and simplifying, we obtain the following equations for the unknown W_x:

$$\mathsf{V}^{\mathrm{T}}\mathsf{H}\mathsf{W}_x = -\mathsf{V}_x^{\mathrm{T}}\mathsf{H}\mathsf{W} + \mathsf{V}^{\mathrm{T}}\mathsf{E}_x\mathsf{W}, \qquad \text{and} \qquad \mathsf{W}^{\mathrm{T}}\mathsf{H}\mathsf{W}_x + \mathsf{W}_x^{\mathrm{T}}\mathsf{H}\mathsf{W} = \mathsf{W}^{\mathrm{T}}\mathsf{E}_x\mathsf{W}.$$

The first matrix equation constitutes $n_{\min}(n - n_{\min})$ scalar equations, while the second equation holds $(n - n_{\min})^2$ scalar equations. Therefore, there are $n(n - n_{\min})$ equations in total. This is precisely the number of degrees of freedom in W_x. Therefore, by choosing those values for W_x that satisfy the matrix equations above, we ensure the antisymmetry of Q_x. $\qquad\square$

Remark 1. *For a given cubature rule, we have shown existence but not uniqueness of an SBP operator. In the proof of Theorem 2, all of the degrees of freedom in W_x were used to satisfy the antisymmetry of Q_x; however, we did not use any of the freedom in the matrices F and G found in E_x. Therefore, in general, there are infinitely many operators associated with a given cubature rule that satisfy Definition 1.*

We now characterize S_x.

Theorem 3. *The matrix S_x of a degree p diagonal-norm multi-dimensional SBP operator is a degree $\tau_{\mathsf{S}_x} = \min\left(\tau_{\mathsf{E}_x}, 2p\right)$ approximation to the bilinear form*

$$(\mathcal{V}, \mathcal{U}) = \int_\Omega \mathcal{V}\frac{\partial\mathcal{U}}{\partial x}\mathrm{d}\Omega \tag{9}$$

Proof. The proof is analogous to the proof in [20] for one-dimensional classical finite-difference-SBP operators. $\qquad\square$

7

Using Theorem ([3](#)) we can characterize Q_x as follows:

Theorem 4. *The matrix Q_x of a degree p diagonal-norm multi-dimensional SBP operator is a degree $\tau_{\mathsf{Q}_x} = \min\left(\tau_{\mathsf{E}_x}, 2p\right)$ approximation to the bilinear form*

$$(\mathcal{V}, \mathcal{U}) = \int_\Omega \mathcal{V} \frac{\partial \mathcal{U}}{\partial x} d\Omega - \frac{1}{2} \oint_\Gamma \mathcal{V}\mathcal{U} d\Gamma \tag{10}$$

Proof. By Theorem ([3](#)) we have that

$$\left(\boldsymbol{x}^{b_x} \circ \boldsymbol{y}^{b_y}\right)^{\mathrm{T}} \mathsf{S}_x \boldsymbol{x}^{a_x} \circ \boldsymbol{y}^{a_y} = \int_\Omega x^{b_x} y^{b_y} \frac{\partial x^{a_x} y^{a_y}}{\partial x} d\Omega, \tag{11}$$

$$\forall \, a_x + a_y + b_x + b_y \le \min\left(\tau_{\mathsf{E}_x}, 2p\right).$$

Substituting $\mathsf{S}_x = \mathsf{Q}_x + \frac{1}{2}\mathsf{E}_x$ into ([11](#)), with rearrangement, gives

$$\left(\boldsymbol{x}^{b_x} \circ \boldsymbol{y}^{b_y}\right)^{\mathrm{T}} \mathsf{Q}_x \boldsymbol{x}^{a_x} \circ \boldsymbol{y}^{a_y} = \int_\Omega x^{b_x} y^{b_y} \frac{\partial x^{a_x} y^{a_y}}{\partial x} d\Omega - \frac{1}{2}\left(\boldsymbol{x}^{b_x} \circ \boldsymbol{y}^{b_y}\right)^{\mathrm{T}} \mathsf{E}_x \boldsymbol{x}^{a_x} \circ \boldsymbol{y}^{a_y}, \tag{12}$$

$$\forall \, a_x + a_y + b_x + b_y \le \min\left(\tau_{\mathsf{E}_x}, 2p\right).$$

Using the definition of E_x we get the desired result

$$\left(\boldsymbol{x}^{b_x} \circ \boldsymbol{y}^{b_y}\right)^{\mathrm{T}} \mathsf{Q}_x \boldsymbol{x}^{a_x} \circ \boldsymbol{y}^{a_y} = \int_\Omega x^{b_x} y^{b_y} \frac{\partial x^{a_x} y^{a_y}}{\partial x} d\Omega - \frac{1}{2} \oint_\Gamma x^{a_x} y^{a_y} x^{b_x} y^{b_y} d\Gamma, \tag{13}$$

$$\forall \, a_x + a_y + b_x + b_y \le \min\left(\tau_{\mathsf{E}_x}, 2p\right).$$

$\square$

4. Constructing the operators

This section describes how we construct diagonal-norm SBP operators for triangles and tetrahedrons. The algorithms described below have been implemented in the Julia package SummationByParts[5].

4.1. The node coordinates and the norm matrix

Theorem [1](#) tells us that the diagonal entries in H are positive weights from a cubature that is exact for polynomials of total degree $2p - 1$. Thus, our first task is to find cubature rules with positive weights for the triangle and tetrahedron. Additionally, we seek rules that use as few nodes as possible for a given accuracy and that respect the symmetries of the triangle and tetrahedron.

For the operators considered in this work, we require that $\binom{p+d-1}{d-1}$ cubature nodes lie on each boundary facet, where d is the spatial dimension. This requirement on the nodes is motivated by the particular form of the E_x, E_y, and E_z operators that we consider below; however, Definition [1](#) does not require a prescribed number of boundary nodes, and SBP operators for the 2- and 3-simplex may exist that do not have any boundary nodes at all.

Table 1: Active orbits and their node counts for triangular-element operators. The notation Perm indicates that every permutation of the barycentric coordinates is to be considered. Free-node counts are decomposed into the product of the number of nodes in the orbit times the number of orbits of that type.

| | orbit name | barycentric form | operator degree, p | | | |
			1	2	3	4
fixed nodes	vertices	$\mathsf{Perm}(1,0,0)$	3	3	3	3
	mid-edge	$\mathsf{Perm}\left(\frac{1}{2},\frac{1}{2},0\right)$	—	3	—	3
	centroid	$\left(\frac{1}{3},\frac{1}{3},\frac{1}{3}\right)$	—	1	—	—
free nodes	edge	$\mathsf{Perm}\left(\alpha,1-\alpha,0\right)$	—	—	6×1	6×1
	S_{21}	$\mathsf{Perm}\left(\alpha,\alpha,1-2\alpha\right)$	—	—	3×1	3×2
		# free parameters	—	—	2	3
		# nodes total	3	7	12	18
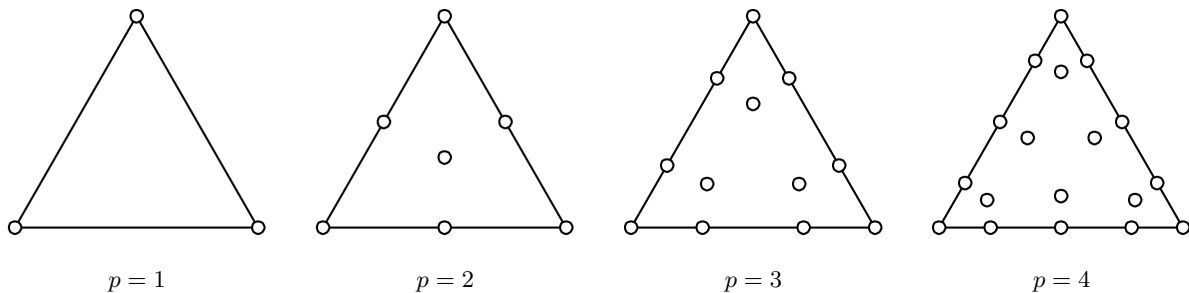
Figure 1: Node distributions for cubature rules adopted for the SBP operators on triangles.

Cubature rules that meet our requirements for triangular elements are presented in references [21–23, 25] in the context of the spectral-element and spectral-difference methods. Table 1 summarizes the rules that are adopted for triangular-element SBP operators of degree $p = 1, 2, 3$, and 4. For reference, the node locations for the triangular cubature rules are shown in Figure 1.

To find cubature rules for the tetrahedron, we follow the ideas presented in [23, 26, 27]. Our procedure is briefly outlined below for completeness, but we make no claims regarding the novelty of the cubature rules or our method of finding them.

We assume that each node belongs to a (possibly degenerate) symmetry orbit [26]. As indicated above, we assume that the cubature-node set includes $p+1$ nodes along each edge and $(p+1)(p+2)/2$ nodes on each triangular face. For the interior nodes, we activate the minimum number of symmetry orbits necessary to satisfy the accuracy conditions; these orbits have been identified through trial-and-error.

Each symmetry orbit has a cubature weight associated with it, and orbits that are non-degenerate are parameterized using one or more barycentric parameters. Together, the orbit parameters and the weights are the degrees of freedom that must be determined. They are found by solving the nonlinear accuracy conditions using the Levenberg-Marquardt algorithm.

9

The accuracy conditions are implemented using the integrals of orthogonal polynomials on the tetrahedron [28, 29].

Table 2 summarizes the node sets used for the tetrahedron cubature rules, and Figure 2 illustrates the node coordinates.

4.2. The boundary operators

Definition 1 implies that the boundary operator E_x satisfies

$$\boldsymbol{v}^{\mathrm{T}}\mathsf{E}_x\boldsymbol{u} = \oint_\Gamma \mathcal{U}\mathcal{V}n_x\, d\Gamma,$$

for all polynomials $\mathcal{U}$ and $\mathcal{V}$ whose total degree is less than $\tau_{\mathsf{E}_x} \geq p$. In particular, if we choose $\mathcal{U}$ and $\mathcal{V}$ to be nodal basis functions on the faces, we can isolate the entries of E_x. This is possible, because we have insisted on operators with $\binom{p+d-1}{d-1}$ nodes on each facet, which leads to a complete nodal basis. For further details on the construction of the boundary operators, we direct the interested reader to [30, pg. 187].

Remark 2. *The boundary operators, when restricted to the boundary nodes, are dense matrices. Contrast this with the tensor-product case, where the boundary operators are diagonal matrices. In the simplex case, we have not found a way to construct diagonal E_x, E_y and E_z that are sufficiently accurate.*

4.3. The antisymmetric part

The accuracy conditions are used to determine the antisymmetric matrices Q_x, Q_y, and Q_z. We will describe the process for Q_x, since it can be adapted in a straightforward way to Q_y and, in the case of the tetrahedron, Q_z.

In theory, we can compute Q_x using the monomials $x^{a_x}y^{a_y}$ that appear in the SBP-operator definition; however, these basis functions are known to produce ill-conditioned Vandermonde matrices. Instead, we follow the standard practice in spectral-element methods and apply the accuracy conditions to appropriate orthogonal bases on the triangle and tetrahedron [28–30]

Let P and P_x be the matrices whose columns are the orthogonal basis function values and derivatives, respectively, evaluated at the nodes. Then the accuracy conditions imply $\mathsf{D}_x\mathsf{P} = \mathsf{P}_x$, or, in terms of the unknown Q_x,

$$\mathsf{Q}_x\mathsf{P} = \mathsf{H}\mathsf{P}_x - \frac{1}{2}\mathsf{E}_x\mathsf{P}.$$

This can be recast as the linear system

$$\mathsf{A}\boldsymbol{q} = \boldsymbol{b}, \tag{14}$$

where $\boldsymbol{q}$ denotes a vector whose entries are the strictly lower part of Q_x:

$$\boldsymbol{q}\left(\tfrac{(i-2)(i-1)}{2} + j\right) = (\mathsf{Q}_x)_{i,j}, \qquad 2 \leq i \leq n, 1 \leq j < i.$$

There are $(n-1)n/2$ unknowns and $n \times \binom{p+d}{d}$ equations in (14); thus, for the operators considered here, there are more equations than unknowns. Fortunately, the compatibility conditions ensure that the system is consistent. Indeed, for $p \geq 3$ the rank of A is actually less than the size of $\boldsymbol{q}$, so there are an infinite number of solutions. In these cases, we choose the minimum-norm least-squares solution [31] to (14).

Table 2: Active orbits and their node counts for tetrahedral-element operators. See the caption of Table 1 for an explanation of the notation.

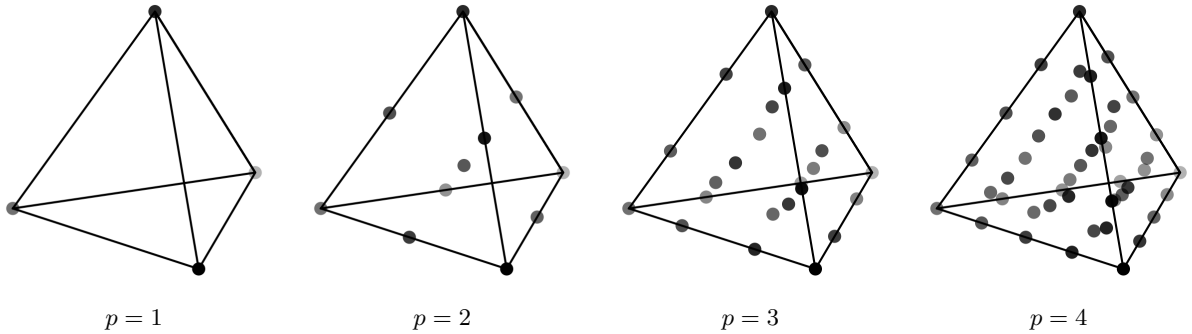|	orbit name	barycentric form	operator degree, p			
			1	2	3	4
fixed nodes	vertices	$\mathsf{Perm}(1,0,0,0)$	4	4	4	4
	mid-edge	$\mathsf{Perm}\left(\frac{1}{2},\frac{1}{2},0,0\right)$	—	6	—	6
	centroid	$\left(\frac{1}{4},\frac{1}{4},\frac{1}{4},\frac{1}{4}\right)$	—	1	—	1
	face centroid	$\mathsf{Perm}\left(\frac{1}{3},\frac{1}{3},\frac{1}{3},0\right)$	—	—	4	—
free nodes	edge	$\mathsf{Perm}\left(\alpha,1-\alpha,0,0\right)$	—	—	12×1	12×1
	face S_{21}	$\mathsf{Perm}\left(\alpha,\alpha,1-2\alpha,0\right)$	—	—	—	12×1
	S_{31}	$\mathsf{Perm}\left(\alpha,\alpha,\alpha,1-3\alpha\right)$	—	—	4×1	4×1
	S_{22}	$\mathsf{Perm}\left(\alpha,\alpha,\frac{1}{2}-\alpha,\frac{1}{2}-\alpha\right)$	—	—	—	6×1
	# free parameters		—	—	2	4
	# nodes total		4	11	24	45

Figure 2: Node distributions for cubature rules adopted for the SBP operators on tetrahedra.

4.4. Similarities and differences with existing operators

There is a vast literature on high-order discretizations for simplex elements, so we focus on the two that share the most in common with the proposed SBP operators: the diagonal mass-matrix spectral-element (SE) method [21–23] and the spectral-difference (SD) method [32].

Our norm matrix H is identical to the lumped mass matrices in the SE method. The difference between the methods arises in the definition of S_x. In the SE method of Giraldo and Taylor [23], the S_x matrix is defined as

$$\left(\mathsf{S}_x^{\mathrm{SE}}\right)_{i,j} = \sum_{k=0}^{n} \mathsf{H}_{k,k} \phi_i(x_k,y_k) \frac{\partial \phi_j}{\partial x}(x_k,y_k),$$

where $\{\phi_i\}_{i=1}^n$ is the so-called cardinal basis. For a degree p operator, the cardinal basis is a

11

polynomial nodal basis that is a super-set of the basis for degree p polynomials; the basis contains polynomials of degree greater than p, because the number of nodes n is greater than $\binom{p+d}{d}$, in general. Consequently, the cubature defined by H is not exact for the product $\phi_i \partial \phi_j / \partial x$ when $p \geq 2$, and the resulting $\mathsf{S}_x^{\mathrm{SE}}$ does not satisfy the SBP definition for the $p \geq 2$ discretizations. Indeed, as the results below demonstrate, the higher-order SE operators are unstable and require filtering or numerical dissipation *even for linear problems.*

Remark 3. *The S_x^{SE} matrix in the diagonal mass-matrix SE method can be made to satisfy the SBP definition by using a cubature rule that is exact for the cardinal basis; however, such a cubature rule would require additional cubature points and would defeat the purpose (i.e. efficiency) of collocating the cubature and basis nodes.*

Diagonal-norm SBP operators can also be viewed as a special case of the SD method in which the unknowns and fluxes are collocated. As pointed out in [32], this means that our proposed SBP operators require more unknowns to achieve a given accuracy than spectral-difference methods; however, collocation eliminates the reconstruction step, so there is a tradeoff between memory and floating-point operations. More importantly, this relative increase in unknowns applies only to discontinuous methods. If we assemble a global SBP operator, as described below, then the number of unknowns can be significantly reduced.

4.5. Assembly of global SBP operators from elemental operators

The SBP operators defined in Sections 4.1–4.3 can be used in a nodal DG formulation [30] with elements coupled weakly using, for example, simultaneous approximation terms [33, 34]. An alternative use for these element-based operators, and the one pursued here, is to mimic the continuous Galerkin formulation. That is, we assemble global SBP operators from the elemental ones.

We need to introduce some additional notation to help describe the assembly process and facilitate the proof of Theorem 5 below. Suppose the domain Ω is partitioned into a set of K non-overlapping subdomains $\Omega^{(k)}$ with boundaries $\Gamma^{(k)}$:

$$\Omega = \bigcup_{k=1}^{K} \bar{\Omega}^{(k)}, \qquad \text{and} \qquad \Omega^{(k)} \cap \Omega^{(l)} = \emptyset, \ \forall \ k \neq l,$$

where $\bar{\Omega}^{(k)} = \Omega^{(k)} \cup \Gamma^{(k)}$ denotes the closure of $\Omega^{(k)}$.

Each subdomain is associated with a set of nodes $S^{(k)} \equiv \{(x_i^{(k)}, y_j^{(k)})\}_{i=1}^{n}$, such that $(x_i^{(k)}, y_i^{(k)}) \in \bar{\Omega}^{(k)}$. In the present context, some of the nodes in $S^{(k)}$ will lie on the boundary $\Gamma^{(k)}$ and be shared by adjacent subdomains.

Let $S \equiv \cup_k S^{(k)}$. Suppose there are n' unique nodes in S, and let each node be assigned a unique global index. Suppose i' is the global index corresponding to the ith local node of element k. We define $\mathsf{Z}^{(k)}(i,j)$ to be the $n' \times n'$ matrix with zeros everywhere except in the (i', j') entry, which is unity. If $e_{i'}$ denotes the i' column of the $n' \times n'$ identity, then $\mathsf{Z}^{(k)}(i,j) = e_{i'} e_{j'}^{\mathrm{T}}$.

We can now state and prove the following result.

Theorem 5. *Let* $\mathsf{D}_x^{(k)} = \left(\mathsf{H}^{(k)}\right)^{-1}\mathsf{S}_x^{(k)}$ *be a degree p SBP operator for the first derivative $\partial/\partial x$ on the node set $S^{(k)}$. If*

$$\mathsf{H} \equiv \sum_{k=1}^{K}\sum_{i=1}^{n}\mathsf{H}_{i,i}^{(k)}\mathsf{Z}^{(k)}(i,i)$$

$$\mathsf{S}_x \equiv \sum_{k=1}^{K}\sum_{i=1}^{n}\sum_{j=1}^{n}\left(\mathsf{S}_x^{(k)}\right)_{i,j}\mathsf{Z}^{(k)}(i,j),$$

then $\mathsf{D}_x = \mathsf{H}^{-1}\mathsf{S}_x$ is a degree p SBP operator on the global node set S.

Proof. We need to check each of the four properties in Definition 1.

i) The first property is straightforward, albeit tedious, to verify. H^{-1} exists by property iii, which is shown to hold independently below, so we have

$$\mathsf{D}_x\boldsymbol{x}^{a_x}\circ\boldsymbol{y}^{a_y} = \mathsf{H}^{-1}\mathsf{S}_x\boldsymbol{x}^{a_x}\circ\boldsymbol{y}^{a_y}$$

$$= \mathsf{H}^{-1}\left[\sum_{k=1}^{K}\sum_{i=1}^{n}\sum_{j=1}^{n}\left(\mathsf{S}_x^{(k)}\right)_{i,j}\mathsf{Z}^{(k)}(i,j)\right]\boldsymbol{x}^{a_x}\circ\boldsymbol{y}^{a_y}$$

$$= \mathsf{H}^{-1}\sum_{k=1}^{K}\sum_{i=1}^{n}\frac{\mathsf{H}_{i,i}^{(k)}}{\mathsf{H}_{i,i}^{(k)}}\sum_{j=1}^{n}\left(\mathsf{S}_x^{(k)}\right)_{i,j}e_{i'}x_{j'}^{a_x}y_{j'}^{a_y}$$

$$= \mathsf{H}^{-1}\sum_{k=1}^{K}\sum_{i=1}^{n}\mathsf{H}_{i,i}^{(k)}e_{i'}\sum_{j=1}^{n}\left(\mathsf{D}_x^{(k)}\right)_{i,j}x_j^{a_x}y_j^{a_y}$$

$$= \mathsf{H}^{-1}\sum_{k=1}^{K}\sum_{i=1}^{n}\mathsf{H}_{i,i}^{(k)}e_{i'}a_x x_i^{a_x-1}y_i^{a_y}$$

$$= \mathsf{H}^{-1}\left[\sum_{k=1}^{K}\sum_{i=1}^{n}\mathsf{H}_{i,i}^{(k)}\mathsf{Z}^{(k)}(i,i)\right]a_x\boldsymbol{x}^{a_x-1}\boldsymbol{y}^{a_y},$$

But the term in brackets above is the definition of H, so we are left with $\mathsf{D}_x\boldsymbol{x}^{a_x}\circ\boldsymbol{y}^{a_y} = a_x\boldsymbol{x}^{a_x-1}\boldsymbol{y}^{a_y}$, as desired.

ii) We form the decomposition $\mathsf{S}_x = \mathsf{Q}_x + \frac{1}{2}\mathsf{E}_x$ where

$$\mathsf{Q}_x = \sum_{k=1}^{K}\sum_{i=1}^{n}\sum_{j=1}^{n}\left(\mathsf{Q}_x\right)^{(k)}(i,j)\mathsf{Z}_{i,j}^{(k)},$$

$$\mathsf{E}_x = \sum_{k=1}^{K}\sum_{i=1}^{n}\sum_{j=1}^{n}\mathsf{E}_x^{(k)}(i,j)\mathsf{Z}_{i,j}^{(k)}.$$

The matrix Q_x is antisymmetric, because it is the sum of antisymmetric matrices. Similarly, E_x is symmetric, because it is the sum of symmetric matrices. Hence, property ii is satisfied.

iii) H is clearly diagonal and positive by construction, so property iii is satisfied.

iv) Finally, property iv can be verified through direct evaluation:

$$(\boldsymbol{x}^{a_x} \circ \boldsymbol{y}^{a_y})^{\mathrm{T}} \, \mathsf{E}_x \boldsymbol{x}^{b_x} \circ \boldsymbol{y}^{b_y} = \sum_{k=1}^{K} \sum_{i=1}^{n} \sum_{j=1}^{n} \mathsf{E}_x^{(k)}(i,j) \, (\boldsymbol{x}^{a_x} \circ \boldsymbol{y}^{a_y}) \, \mathsf{Z}_{i,j}^{(k)} \boldsymbol{x}^{b_x} \circ \boldsymbol{y}^{b_y}$$

$$= \sum_{k=1}^{K} \oint_{\Gamma^{(k)}} x^{a_x+b_x} y^{a_y+b_y} n_x \mathrm{d}\Gamma$$

$$= \oint_{\Gamma} x^{a_x+b_x} y^{a_y+b_y} n_x \mathrm{d}\Gamma,$$

where we have used the fact that the boundary fluxes of adjacent elements cancel analytically.

$\square$

5. Results

The linear advection equation is used to verify and study the triangular-element SBP operators of Section 4. In particular, we consider the problem

$$\frac{\partial \mathcal{U}}{\partial t} + \frac{\partial \mathcal{U}}{\partial x} + \frac{\partial \mathcal{U}}{\partial y} = 0, \qquad \forall \, (x,y) \in \Omega = [0,1]^2,$$

$$\mathcal{U}(x,0,t) = \mathcal{U}(x,1,t), \qquad \text{and} \qquad \mathcal{U}(0,y,t) = \mathcal{U}(1,y,t),$$

$$\mathcal{U}(x,y,0) = \begin{cases} 1 - (4r^2 - 1)^5 & \text{if } r \leq \frac{1}{2} \\ 1, & \text{otherwise,} \end{cases}$$

where $r(x,y) \equiv \sqrt{(x-\frac{1}{2})^2 + (y-\frac{1}{2})^2}$. The boundary conditions imply periodicity in both the x and y directions and the PDE implies an advection velocity of $(1,1)$. The initial condition is a C^4 continuous bump function that is periodic on Ω.

A nonuniform mesh for the square domain Ω is generated, in order to eliminate possible error cancellations that may arise on uniform grids. The vertices of the mesh are given by

$$x_{i,j} = \frac{i}{N} + \frac{1}{40} \sin\left(2\pi i/N\right) \sin\left(2\pi j/N\right), \qquad y_{i,j} = \frac{j}{N} + \frac{1}{40} \sin\left(2\pi i/N\right) \sin\left(2\pi j/N\right),$$

where N is the number of elements along an edge, and $i,j = 0,1,2,\ldots,N$. The nominal element size is $h \equiv 1/N$. A triangular mesh is generated by dividing each quadrilateral $\{x_{i,j}, x_{i+1,j}, x_{i,j+1}, x_{i+1,j+1}\}$ along the diagonal from $x_{i+1,j}$ to $x_{i,j+1}$. Finally, for an SBP element of degree p, the reference-element nodes are mapped (affinely) to each triangle in the mesh. Figure 3 illustrates a representative mesh for $p = 3$ and $N = 12$.

The global SBP operators are constructed using the assembly process described in Section 4.5. Appropriate coordinate transformations are used to adapt the reference-element SBP operators to each triangle in the mesh. In addition, the periodic boundaries are transparent to the operator, that is, nodes that coincide on the periodic boundary are considered the same.

The classical 4th-order Runge-Kutta scheme is used to discretize the time derivative. The maximally stable CFL number for each SBP operator was identified for $N = 32$ using Golden-Section optimization, where the CFL number was defined as $\sqrt{2}\Delta t/h$ for a time-step size of Δt. Each discretization was run for a period of $T = 1$ and considered stable if the final L^2 norm of the solution was less than the initial solution norm. The results of the optimization are listed in Table 3.

Table 3: Maximally stable CFL numbers for the SBP operators on the nonuniform mesh with $N = 32$.

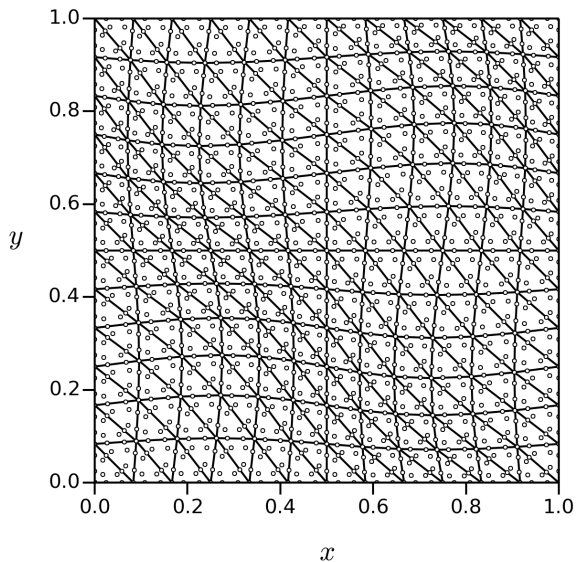|	p=1	p=2	p=3	p=4
CFL_{max}	1.885	0.532	0.270	0.149

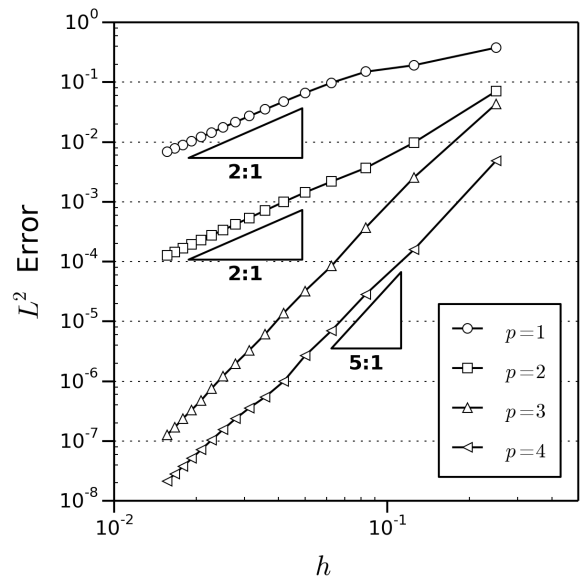Figure 3: Example mesh with $p = 3$ and $N = 12$ for accuracy and energy-norm studies.

Figure 4: L^2 error between the solution at $t = 1$ and initial condition for different mesh spacing and operators.

5.1. Accuracy and efficiency studies

Figure 4 plots the L^2 error between the initial condition and the final solution at $t = 1$ (i.e. one period) for SBP-operator degrees one to four and a range of N. Specifically, if $\boldsymbol{u}_0$ and $\boldsymbol{u}$ are the discrete initial and final solutions, respectively, and H is the SBP norm on the global domain, then the error is

$$L^2 \text{ Error} = \sqrt{(\boldsymbol{u} - \boldsymbol{u}_0)^{\mathrm{T}} \mathsf{H} (\boldsymbol{u} - \boldsymbol{u}_0)}.$$

The mesh resolution ranges from $N = 4$ to $N = 64$ in increments of 4. Each case was time marched using $\text{CFL}_{\text{max}}/2$, which was determined to be sufficiently small to produce negligible temporal discretization errors.

The results in Figure 4 demonstrate relative improvement when the operator degree is increased; however, the convergence rates of the $p = 2$ and $p = 4$ operators appear to be lower than the expected asymptotic rates, and the convergence rate of the $p = 3$ operator is higher than expected. Giraldo and Taylor also observed convergence rates that were inconsistent with the expected rates when the diagonal mass matrix triangular spectral-element method was applied to linear advection on the sphere. The root cause of these unexpected convergence rates is unclear and will be the focus of future work.

Figure 5 plots the L^2 error, normalized by the L^2 norm of the initial condition, versus CPU time. The runs were performed on an Intel® Core i5-3570K processor and the code was implemented in
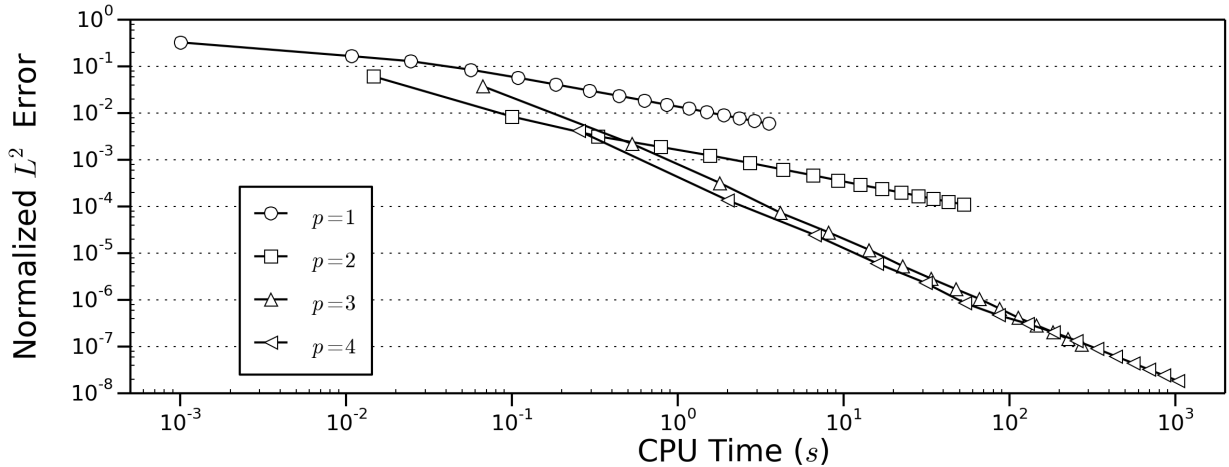
Figure 5: Normalized L^2 error at $T = 1$ versus CPU time measured in seconds.

Julia version 0.4.0. For this problem, the $p = 2$ SBP discretization is the most efficient over the range of accuracies typical of engineering applications. When the desired relative accuracy is below 0.3%, the $p = 4$ discretization is the most efficient. These results are typical of other high-order discretizations applied to linear convection.

5.2. Stability studies

Figure 6 shows the spectra of the SBP and SE spatial operators for the linear advection problem. Specifically, these eigenvalues are for the global operator $\mathsf{S}_x + \mathsf{S}_y$ when $N = 12$. The eigenvalues of the SBP operators are imaginary to machine precision, which mimics the continuous spectrum for this periodic problem. This is as expected, because the boundary operators $\mathsf{E}_x^{(k)}$ cancel between adjacent elements when the SBP derivative operator is assembled, leaving only the antisymmetric parts. The SE operator for $p = 1$ also has a purely imaginary spectrum, because it is identical to the linear SBP operator; however, the spectra of the high-order SE operators have a real component.

The consequences of the eigenvalue distributions are evident when the linear advection problem is integrated for two periods. Figure 7 plots the difference between the solution L^2 norm at time $t \in [0, 2]$ and the initial solution norm, i.e. the change in "energy",

$$\Delta E = \boldsymbol{u}_n^{\mathrm{T}} \mathsf{H} \boldsymbol{u}_n - \boldsymbol{u}_0^{\mathrm{T}} \mathsf{H} \boldsymbol{u}_0,$$

where $\boldsymbol{u}_n$ denotes the discrete solution at time step n. For this study, $N = 12$ and the CFL number was fixed at 0.01 to reduce temporal errors.

The energy history in Figure 7 clearly shows that the SE operators are unstable for this linear advection problem, while the SBP operators are stable. The small (linear) decrease in the SBP energy error is due to temporal errors and can be eliminated by using a different time-marching method, e.g. leapfrog, or at the cost of using a sufficiently small CFL number.

6. Conclusions

We proposed a definition for multidimensional SBP operators that is a natural extension of the classical one-dimensional SBP operator definition. We studied the theoretical implications of the
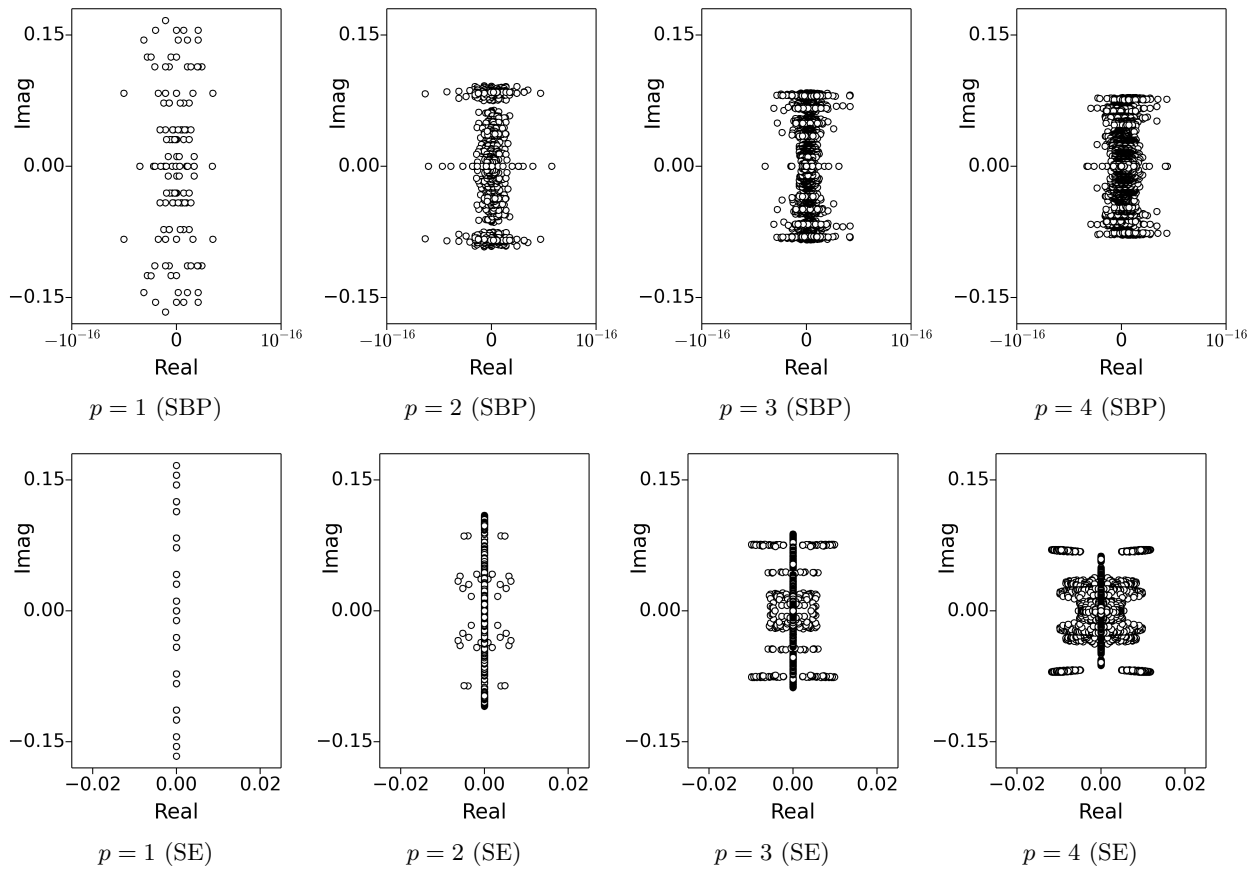
16

Figure 6: Eigenvalue distributions for the SBP (upper row) and the SE (lower row) spatial discretizations of the linear advection problem. Note the different ranges for the real variables.
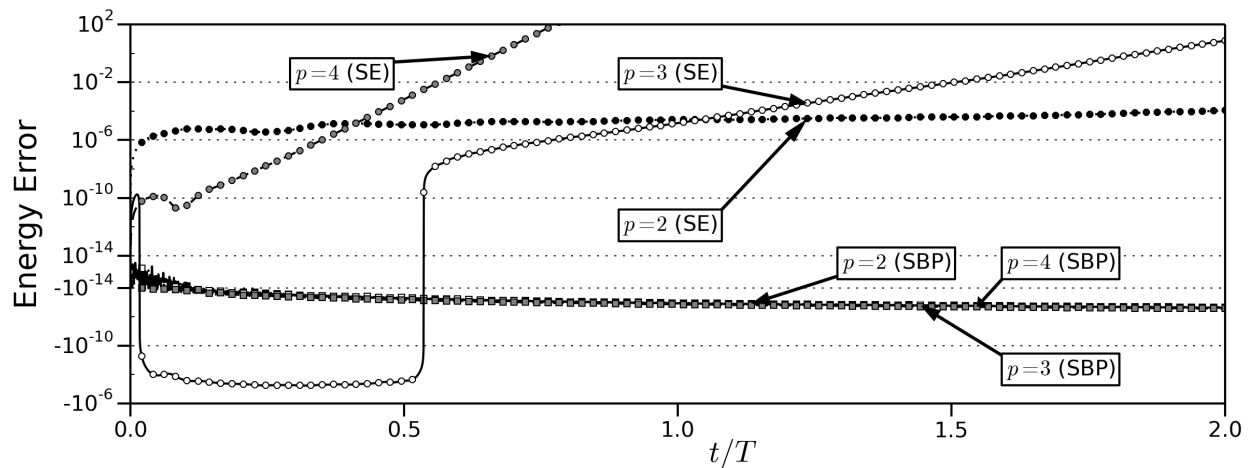

Figure 7: Time history of the change in the solution energy norm. Note the use of a symmetric logarithmic scale on the vertical axis.

17

definition in the case of diagonal-norm operators, and showed that the generalized operators retain the attractive properties of tensor-product SBP operators. A significant theoretical result of this work is that, for a given domain, a cubature rule with positive weights is necessary and sufficient for the existence of diagonal-norm SBP operators on that domain.

We also constructed diagonal-norm SBP operators for the triangle and tetrahedron. To the best of our knowledge, this is the first example of SBP operators of degree $p \geq 2$ on these domains. We also presented an assembly procedure that constructs SBP operators for a global domain from element-wise SBP operators.

Finally, we verified the triangle-element SBP operators using linear advection on a doubly periodic domain. The results demonstrate the time stability and accuracy of the operators. The results suggest these operators could be effective for the long-time simulation of turbulent flows on complex domains.

Acknowledgments

References

[1] Kreiss, H.-O. and Scherer, G., "Finite element and finite difference methods for hyperbolic partial differential equations," *Mathematical aspects of finite elements in partial differential equations*, Academic Press, New York/London, 1974, pp. 195–212.

[2] Carpenter, M. H., Nordström, J., and Gottlieb, D., "A stable and conservative interface treatment of arbitrary spatial accuracy," *Journal of Computational Physics*, Vol. 148, No. 2, 1999, pp. 341–365.

[3] Yee, H. C. and Sjögreen, B., "Designing adaptive low-dissipative high order schemes for long-time integrations," *Turbulent Flow Computation*, Springer, 2002, pp. 141–198.

[4] Nordström, J., "Conservative finite difference formulations, variable coefficients, energy estimates and artificial dissipation," *Journal of Scientific Computing*, Vol. 29, 2006, pp. 375–404.

[5] Morinishi, Y., Lund, T. S., Vasilyev, O. V., and Moin, P., "Fully Conservative Higher Order Finite Difference Schemes for Incompressible Flow," *Journal of Computational Physics*, Vol. 143, 1998, pp. 90–124.

[6] Yee, H. C., Vinokur, M., and Djomehri, M. J., "Entropy Splitting and Numerical Dissipation," *Journal of Computational Physics*, Vol. 162, No. 1, July 2000, pp. 33–81.

[7] Strand, B., "Summation by parts for finite difference approximations for d/dx," *Journal of Computational Physics*, Vol. 110, No. 1, 1994, pp. 47–67.

[8] Mattsson, K. and Nordström, J., "Summation by parts operators for finite difference approximations of second derivatives," *Journal of Computational Physics*, Vol. 199, No. 2, 2004, pp. 503–540.

[9] Svärd, M., "On coordinate transformations for summation-by-parts operators," *Journal of Scientific Computing*, Vol. 20, No. 1, Feb. 2004, pp. 29–42.

[10] Mattsson, K., "Summation by Parts Operators for Finite Difference Approximations of Second-Derivatives with Variable Coefficients," *Journal of Scientific Computing*, Vol. 51, No. 3, June 2012, pp. 650–682.

[11] Svärd, M., Mattsson, K., and Nordström, J., "Steady-State Computations Using Summation-by-Parts Operators," *Journal of Scientific Computing*, Vol. 24, No. 1, July 2005, pp. 79–95.

[12] Hicken, J. E. and Zingg, D. W., "A parallel Newton-Krylov solver for the Euler equations discretized using simultaneous approximation terms," *AIAA Journal*, Vol. 46, No. 11, Nov. 2008, pp. 2773–2786.

[13] Nordström, J., Gong, J., van der Weide, E., and Svärd, M., "A stable and conservative high order multi-block method for the compressible Navier-Stokes equations," *Journal of Computational Physics*, Vol. 228, No. 24, 2009, pp. 9020–9035.

[14] Kitson, A., McLachlan, R. I., and Robidoux, N., "Skew-adjoint finite difference methods on nonuniform grids," *New Zealand Journal of Mathematics*, Vol. 32, No. 2, 2003, pp. 139–159.

[15] Kwan-yu Chiu, E., Wang, Q., Hu, R., and Jameson, A., "A Conservative Mesh-Free Scheme and Generalized Framework for Conservation Laws," *SIAM Journal on Scientific Computing*, Vol. 34, No. 6, Jan. 2012, pp. A2896–A2916.

[16] Chiu, E. K., Wang, Q., and Jameson, A., "A conservative meshless scheme: general order formulation and application to Euler equations," *49th AIAA Aerospace Sciences Meeting*, No. AIAA–2011–651, Orlando, Florida, Jan. 2011.

[17] Carpenter, M. H. and Gottlieb, D., "Spectral methods on arbitrary grids," *Journal of Computational Physics*, Vol. 129, No. 1, 1996, pp. 74–86.

[18] Gassner, G. J., "A skew-symmetric discontinuous Galerkin spectral element discretization and its relation to SBP-SAT finite difference methods," *SIAm Journal on Scientific Computing*, Vol. 35, No. 3, 2013, pp. A1233–A1253.

[19] Del Rey Fernández, D. C., Boom, P. D., and Zingg, D. W., "A Generalized Framework for Nodal First Derivative Summation-By-Parts Operators," *Journal of Computational Physics*, Vol. 266, No. 1, 2014, pp. 214–239.

[20] Hicken, J. E. and Zingg, D. W., "Summation-by-parts operators and high-order quadrature," *Journal of Computational and Applied Mathematics*, Vol. 237, No. 1, 2013, pp. 111–125.

[21] Cohen, G., Joly, P., Roberts, J. E., and Tordjman, N., "Higher Order Triangular Finite Elements with Mass Lumping for the Wave Equation," *SIAM Journal on Numerical Analysis*, Vol. 38, No. 6, Jan. 2001, pp. 2047–2078.

[22] Mulder, W. A., "Higher-order mass-lumped finite elements for the wave equation," *Journal of Computational Acoustics*, Vol. 09, No. 02, June 2001, pp. 671–680.

[23] Giraldo, F. X. and Taylor, M. A., "A diagonal-mass-matrix triangular-spectral-element method based on cubature points," *Journal of Engineering Mathematics*, Vol. 56, No. 3, 2006, pp. 307–322.

[24] Hicken, J. E. and Zingg, D. W., "Dual consistency and functional accuracy: a finite-difference perspective," *Journal of Computational Physics*, Vol. 256, Jan. 2014, pp. 161–182.

[25] Liu, Y. and Vinokur, M., "Exact Integrations of Polynomials and Symmetric Quadrature Formulas over Arbitrary Polyhedral Grids," *Journal of Computational Physics*, Vol. 140, No. 1, 1998, pp. 122–147.

[26] Zhang, L., Cui, T., and Liu, H., "A Set of Symmetric Quadrature Rules on Triangles and Tetrahedra," *Journal of Computational Mathematics*, Vol. 27, No. 1, 2009, pp. 89–96.

[27] Witherden, F. D. and Vincent, P. E., "On the Identification of Symmetric Quadrature Rules for Finite Element Methods," Sept. 2014.

[28] Koornwinder, T., "Two-variable analogues of the classical orthogonal polynomials," *Theory and application of special functions*, Academic Press New York, 1975, pp. 435–495.

[29] Dubiner, M., "Spectral methods on triangles and other domains," *Journal of Scientific Computing*, Vol. 6, No. 4, 1991, pp. 345–390.

[30] Hesthaven, J. S. and Warburton, T., *Nodal discontinuous Galerkin methods: algorithms, analysis, and applications*, Springer-Verlag, New York, 2008.

[31] Golub, G. H. and Van Loan, C. F., *Matrix Computations*, The John Hopkins University Press, 3rd ed., 1996.

[32] Liu, Y., Vinokur, M., and Wang, Z. J., "Spectral difference method for unstructured grids I: Basic formulation," *Journal of Computational Physics*, Vol. 216, No. 2, Aug. 2006, pp. 780–801.

[33] Funaro, D. and Gottlieb, D., "A new method of imposing boundary conditions in pseudospectral approximations of hyperbolic equations," *Mathematics of Computation*, Vol. 51, No. 184, Oct. 1988, pp. 599–613.

[34] Carpenter, M. H., Gottlieb, D., and Abarbanel, S., "Time-stable boundary conditions for finite-difference schemes solving hyperbolic systems: Methodology and application to high-order compact schemes," *Journal of Computational Physics*, Vol. 111, No. 2, 1994, pp. 220–236.

[35] Hunter, J. D., "Matplotlib: A 2D graphics environment," *Computing In Science & Engineering*, Vol. 9, No. 3, 2007, pp. 90–95.